

1 **Supplemental Information:** Atmospheric Fates of Criegee Intermediates in the Ozonolysis of
2 Isoprene

3 Tran B. Nguyen,^{10*} Geoffrey S. Tyndall,² John D. Crouse,¹ Alexander P. Teng,¹ Kelvin H. Bates,³
4 Rebecca H. Schwantes,¹ Matthew M. Coggon,^{3φ} Li Zhang,⁵ Philip Feiner,⁵ David O. Miller,⁵ Kate
5 M. Skog,⁶ Jean C. Rivera-Rios,^{6ξ} Matthew Dorris,⁶ Kevin F. Olson,^{7,8ψ} Abigail Koss,⁹ Robert J.
6 Wild,^{9,10} Steven S. Brown,⁹ Allen H. Goldstein,^{7,8} Joost A. de Gouw,⁹ William H. Brune,⁵ Frank
7 N. Keutsch,^{6ξ} John H. Seinfeld,^{3,4} and Paul O. Wennberg^{1,4}

8

9 1. Division of Geological and Planetary Sciences, California Institute of Technology, Pasadena,
10 California, USA

11 2. Atmospheric Chemistry Observations & Modeling Laboratory, National Center for Atmospheric
12 Research, Boulder, CO, USA

13 3. Division of Chemistry and Chemical Engineering, California Institute of Technology, Pasadena,
14 California, USA

15 4. Division of Engineering and Applied Science, California Institute of Technology, Pasadena, California,
16 USA

17 5. Department of Meteorology, The Pennsylvania State University, University Park, PA, USA

18 6. Department of Chemistry, University of Wisconsin at Madison, Madison, WI, USA

19 7. Department of Environmental Science, Policy, and Management, University of California at Berkeley,
20 Berkeley, CA, USA

21 8. Department of Civil and Environmental Engineering, University of California at Berkeley, Berkeley,
22 CA, USA

23 9. Earth Systems Research Laboratory, Chemical Sciences Division, National Oceanographic and
24 Atmospheric Association, Boulder, CO, USA

25 10. Cooperative Institute for Research in Environmental Sciences, University of Colorado, Boulder, CO,
26 USA

27 ^θ Now at Dept. of Environmental Toxicology, University of California, Davis, Davis, CA

28 ^φ Now at Earth Systems Research Laboratory, Chemical Sciences Division, National Oceanographic and
29 Atmospheric Association, Boulder, CO, USA

30 ^ξ Now at Department of Chemistry and Chemical Biology, Harvard University, Cambridge, MA, USA

31 ^ψ Now at Chevron Corp, San Ramon, CA, USA

32

33 **author to whom correspondence should be directed: tbn@ucdavis.edu*

1 **Table S1:** Detection and quantification of compounds using negative-ion CF_3O^- CIMS.

2

Chemical Name (abbrev.)	Chemical Formula	MS stage	Ion m/z	Ionic composition	Quantification method	Water dependence
Water vapor	H_2O	1	104	$^{13}\text{CF}_3\text{O}\cdot(\text{H}_2\text{O})^-$	FT-IR	V. Strong
		1	121	$\text{CF}_3\text{O}\cdot(\text{H}_2\text{O})_2^-$	FT-IR	V. Strong
Acetic acid (AA)	$\text{CH}_3\text{C}(\text{O})\text{OH}$	1	79	$\text{HF}\cdot[\text{O}(\text{O})\text{CCH}_3]^-$	Gravimetric	Strong
		2	145 → 79	$\text{CF}_3\text{O}\cdot[\text{AA}]^- \rightarrow$ $\text{HF}[\text{O}(\text{O})\text{CCH}_3]^-$	Gravimetric	Strong
Formic acid	$\text{HC}(\text{O})\text{OH}$	1	65	$\text{HF}\cdot(\text{O}(\text{O})\text{CH})^-$	Gravimetric	Strong
Nitric acid	HNO_3	1	82	$\text{HF}\cdot(\text{ONO}_2)^-$	Gravimetric	Weak
Peracetic acid (PAA)	$\text{CH}_3\text{C}(\text{O})\text{OOH}$	1	161	$\text{CF}_3\text{O}\cdot(\text{PAA})^-$	Colorimetric (UV-Vis)	Moderate
		1	119	$\text{CF}_3\text{O}\cdot(\text{HOOH})^-$	Colorimetric (UV-Vis)	Strong
Hydrogen peroxide	HOOH	2	119 → 85	$\text{CF}_3\text{O}\cdot(\text{HOOH}) \rightarrow$ CF_3O^-	Colorimetric (UV-Vis)	Strong
		2	133 → 85	$\text{CF}_3\text{O}\cdot(\text{CH}_3\text{OOH})^-$	Colorimetric (UV-Vis)	Strong
Methyl hydroperoxide (MHP)	CH_3OOH	2	133 → 85	$\text{CF}_3\text{O}\cdot(\text{CH}_3\text{OOH})^-$	Colorimetric (UV-Vis)	Strong
Hydroxymethyl hydroperoxide (HMHP)	HOCH_2OOH	1	149	$\text{CF}_3\text{O}\cdot(\text{HMHP})^-$	FT-IR	Weak
Hydroxyacetone (HAC)	$\text{HOCH}_2\text{C}(\text{O})\text{CH}_3$	1	159	$\text{CF}_3\text{O}\cdot(\text{HAC})^-$	Gravimetric	Weak
Glycolaldehyde (GLYC)	$\text{HOCH}_2\text{C}(\text{O})\text{H}$	1	145 →	$\text{CF}_3\text{O}\cdot(\text{GLYC})^-$	FT-IR	Weak
		2	85	$\rightarrow\text{CF}_3\text{O}^-$		

3

4

1 **Scheme S1:** Model mechanism at T= 295 K and P = 1 atm, based on a condensed version of Figure 4 in the
2 main text. The OH chemistry of cyclohexane (CHX) is monitored as it produces RO₂ and consumes HO₂.
3 Standard background chemistry (e.g., HO_x, NO_y reactions, not shown) is also incorporated. Minor
4 oxygenated organics (e.g., 1-hydroperoxy-2-oxy-but-3-ene) are all lumped as a generic “product”
5 compound. Rate coefficients for the background reactions are based off IUPAC recommendations except
6 where noted.

7
8
9

10

11 **Ozone and OH Mechanism for Isoprene, MACR, MVK, CHX**

12

13 x34POZ=0.6;

14 x12POZ=0.4;

15 xMACR=0.68;

16 xMACROO=1-xMACR;

17 xsynMACROO=0.2;

18 xantiMACROO=0.8;

19 xMVK=0.42;

20 xMVKOO = 1-xMVK;

21 xsynMVKOO=0.6;

22 xantiMVKOO=0.4;

23 xdioxole=0.25;

24 xdioxirane=0.72;

25 xstable =0.03;

26 xdecarbox = 0.7;

27 xPA_CH3CH2 = 0.35;

28 xHP = 0.3;

29 xDC = 0.3;

30 xRO = 0.4;

31

32 xOH=x12POZ.*xMVKOO.*xsynMVKOO;

33 yOH = xOH ...

34 + xOH.*xRO + xOH.*xDC + xOH.*xRO.*xRO...

35 + x34POZ.*xMACROO.*xantiMACROO.*xdioxirane.*xdecarbox.*xRO.*xPA_CH3CH2...

36 + x34POZ.*xMACROO.*xsynMACROO.*xdioxirane.*xdecarbox.*xRO.*xPA_CH3CH2...

37 + x12POZ.*xMVKOO.*xantiMVKOO.*xdioxirane.*xdecarbox.*xRO.*xPA_CH3CH2;

38

39 yform= (x34POZ.*xMACROO + x12POZ.*xMVKOO)...

40 + xOH.*xRO + xOH.*xRO.*xRO ...

41 + x34POZ.*xMACROO.*xantiMACROO.*xdioxirane.*xdecarbox...

42 + x34POZ.*xMACROO.*xsynMACROO.*xdioxirane.*xdecarbox ...

43 + x12POZ.*xMVKOO.*xantiMVKOO.*xdioxirane.*xdecarbox;

44

45 yHO2 = xOH.*xDC + xOH.*xRO.*xRO ...

46 + x34POZ.*xMACROO.*xantiMACROO.*xdioxirane.*xdecarbox...

47 + x34POZ.*xMACROO.*xsynMACROO.*xdioxirane.*xdecarbox;

48

49 ymacr=x34POZ.*xMACR;

50 ymvk=x12POZ.*xMVK;

51

52 **Isop + O3;**

53 k=1.3e-17;

54 Y(MACR) = ymacr;

55 Y(MVK) = ymvk;

56 Y(HCHO) = yform;

```

1 Y(CH2OO_SCI) = ymacr + ymvk;
2 Y(MACROO_SCI) = x34POZ.*xMACROO.*xstable;
3 Y(MVKOO_SCI) = x12POZ.*xMVKOO.*xstable;
4 Y(OH) = yOH
5 Y(HO2) = yHO2;
6 Y(products) = xOH*xHP + xOH.*xDC + xOH.*xRO +
7 x34POZ.*xMACROO.*xantiMACROO.*xdioxole +
8 x12POZ.*xMVKOO.*xantiMVKOO.*xdioxole;
9
10 MACR + O3;
11 k=1.8e-18;
12 Y(products) = 1;
13
14 MVK + O3;
15 k=4.8e-18;
16 Y(products) = 1;
17
18 Isop + OH;
19 k=1e-10;
20 Y(products) = 1;
21
22 MACR + OH;
23 k=3.4e-11;
24 Y(products) = 1;
25
26 MACR + OH;
27 k=1.9e-11;
28 Y(products) = 1;
29
30 CHX + OH;
31 k=7.3e-12;
32 Y(CHX_RO2) = 1;
33
34 CHX_RO2 + CHX_RO2;
35 k=5.7e-12;
36 Y(cyclohexanone) = 0.5;
37 Y(cyclohexanol) = 0.5;
38
39 CHX_RO2 + HO2;
40 k= 1.612e-11;
41 Y(cyclohexane hydroperoxide) = 1;
42
43 CHX_RO2 + SCI;
44 k= 5e-12;
45 Y(products) = 1;
46
47 CH2OO_SCI + H2O;
48 k=0.9e-15;
49 Y(HMHP) = 0.73;
50 Y(H2O2) = 0.06;
51 Y(HCHO) = 0.06;
52 Y(HCOOH) = 0.21;
53
54 CH2OO_SCI + (H2O)2;
55 k=0.8e-12;
56 Y(HMHP) = 0.40;
57 Y(H2O2) = 0.06;

```

```

1 Y(HCHO) = 0.06;
2 Y(HCOOH) = 0.54;
3
4 CH2OO_SCI + Isop;
5 k=1.78e-13;
6 Y(products) = 1;
7
8 CH2OO_SCI + O3;
9 k=1e-12;
10 Y(HCHO) = 0.7;
11
12 MACROO_SCI + H2O;
13 k=1.8e-15;
14 Y(products) = 1;
15
16 MACROO_SCI;
17 k=250;
18 Y(products) = 1;
19
20 MVKOO_SCI + H2O;
21 k=1.8e-15;
22 Y(products) = 1;
23
24 MVKOO_SCI;
25 k=250;
26 Y(products) = 1;
27
28
29 

---


30 Background Mechanism
31 HO2 + HO2;      %water dependent, k based on Stone and Rowley PCCP 2005
32 k= 1.8e-14.*exp(1500/T)*(1+1e-25.*fH2O.*M.*exp(4670/T));
33 Y(H2O2) = 1;
34 Y(O2) = 1;
35
36 OH + H2O2;
37 k= 1.69e-12;
38 Y(H2O) = 1;
39 Y(HO2) = 1;
40
41 OH + HO2;
42 k= 1e-10;
43 Y(H2O) = 1;
44 Y(O2) = 1;
45
46 OH + OH;
47 k0=7.0e-31.*(T./300).^(-1);
48 kinf=2.6e-11.*(T./300).^(-0);
49 Fc=0.6;
50 k=(k0.*M)./(1+(k0.*M./kinf)).*Fc.^((1+(log10(k0.*M./kinf)).^2).^(-1));
51 Y(H2O2) = 1;
52
53 OH + HONO;
54 k0=7.0e-31.*(T./300).^(-1);
55 kinf=2.6e-11.*(T./300).^(-0);
56 Fc=0.6;
57 k=(k0.*M)./(1+(k0.*M./kinf)).*Fc.^((1+(log10(k0.*M./kinf)).^2).^(-1));

```

```

1 Y(H2O) = 1;
2 Y(H2O2) = 1;
3
4 OH + HNO3;
5 k0=2.4e-14*exp(460/T);
6 k2=2.7e-17*exp(2199/T);
7 k3=6.5e-34*exp(1335/T);
8 k=k0+k3.*M./(1+k3.*M./k2);
9 Y(H2O) = 1;
10 Y(NO3) = 1;
11
12 OH + NO;
13 k0=7.0e-31.*(T./300).^(-2.6);
14 kinf=3.6e-11.*(T./300).^(-0.1);
15 k=k0.*M./(1+(k0.*M./kinf)).*0.6.^((1+(log10(k0.*M./kinf)).^2).^(-1));
16 Y(HONO) = 1;
17
18 OH + NO2;
19 k0=1.51e-30.*(T./300).^(-3.0); % Updated to Mollner, Science, 2010
20 kinf=2.58e-11.*(T./300).^(-0.0);
21 k=k0.*M./(1+(k0.*M./kinf)).*0.6.^((1+(log10(k0.*M./kinf)).^2).^(-1));
22 Y(HNO3) = 1;
23
24 OH + NO2;
25 k0=6.2e-32.*(T./300).^(-3.9);
26 kinf=8.1e-11.*(T./300).^(-0.5);
27 k=k0.*M./(1+(k0.*M./kinf)).*0.6.^((1+(log10(k0.*M./kinf)).^2).^(-1));
28 Y(HOONO) = 1;
29
30 HOONO;
31 eq=3.9e-27.*exp(10125./T);
32 k0=6.2e-32.*(T./300).^(-3.9);
33 kinf=8.1e-11.*(T./300).^(-0.5);
34 kf=k0.*M./(1+(k0.*M./kinf)).*0.6.^((1+(log10(k0.*M./kinf)).^2).^(-1));
35 k=kf/eq;
36 Y(HO) = 1;
37 Y(NO2) = 1;
38
39 HO2 + NO;
40 k=8.17E-12;
41 Y(OH) = 1;
42 Y(NO2) = 1;
43
44 O(3P) + HO2;
45 k= 5.9e-11;
46 Y(OH) = 1;
47 Y(O2) = 1;
48
49 O(3P) + O2;
50 k= 6.0e-34*(T/300)^(-2.4)*M;
51 Y(O3) = 1;
52
53 O3 + HO2;
54 k= 1.9e-15;
55 Y(OH) = 1;
56 Y(O2) = 2;
57

```

```

1 O3 + OH;
2 k= 7e-14;
3 Y(HO2) = 1;
4 Y(O2) = 1;
5
6 O(1D) + H2O;
7 k= 2e-10;
8 Y(OH) = 2;
9
10 O(1D);
11 k= 3.2e-11*exp(67/T)*M;
12 Y(O3P) = 1;
13
14 O(3P) + NO;
15 k0=9.0e-32.*(T./300).^(-1.5);
16 kinf=3.0e-11.*(T./300).^(-0.0);
17 k=k0.*M./(1+(k0.*M./kinf)).*0.6.^((1+(log10(k0.*M./kinf)).^2).^(-1));
18 Y(NO2) = 1;
19
20 O(3P) + NO2;
21 k= 1.04e-11;
22 Y(NO) = 1;
23 Y(O2) = 1;
24
25 O(3P) + NO2;
26 k0=2.5e-31.*(T./300).^(-1.8);
27 kinf=2.2e-11.*(T./300).^(-0.7);
28 k=k0.*M./(1+(k0.*M./kinf)).*0.6.^((1+(log10(k0.*M./kinf)).^2).^(-1));
29 Y(NO3) = 1;
30
31 O3 + NO;
32 k=1.86e-14;
33 Y(NO2) = 1;
34 Y(O2) = 1;
35
36 O3 + NO + NO;
37 k= 2e-38.*cO2;
38 Y(NO) = 1;
39 Y(NO3) = 1;
40
41 O3 + NO2;
42 k= 3.46e-11;
43 Y(NO3) = 1;
44 Y(O2) = 1;
45
46 NO3 + NO2;
47 k0=2.7e-27.*(T./300).^(-4.4);
48 kinf=1.4e-12.*(T./300).^(-0.7);
49 k=k0.*M./(1+(k0.*M./kinf)).*0.6.^((1+(log10(k0.*M./kinf)).^2).^(-1));
50 Y(N2O5) = 1;
51
52 N2O5 + H2O;
53 k= 2.5e-22;
54 Y(HNO3) = 2;
55
56 N2O5 + H2O + H2O;
57 k= 1.8E-39*fH2O*M;

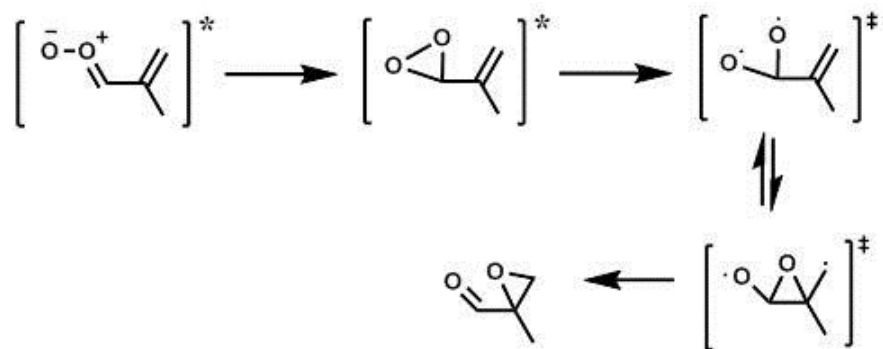
```

```

1 Y(HNO3) = 2;
2 Y(H2O) = 1;
3
4 N2O5;
5 eq=2.7e-27.*exp(11000./T);
6 k0=9.0e-29.*(T./300).^(-4.4);
7 kinf=1.4e-12.*(T./300).^(-0.7);
8 kf=k0.*M./(1+(k0.*M./kinf)).*0.6.^((1+(log10(k0.*M./kinf)).^2).^(-1));
9 k=kf/eq;
10 Y(NO3) = 1;
11 Y(NO2) = 1;
12
13 NO3 + NO;
14 k= 2.27e-11;
15 Y(NO2) = 2;
16
17 NO3 + NO3;
18 k= 2.1e-16;
19 Y(NO2) = 2;
20 Y(O2) = 1;
21
22 NO3 + HO2;
23 k= 3.5e-12;
24 Y(NO2) = 1;
25 Y(O2) = 1;
26 Y(OH) = 1;
27
28 HO2 + NO2;
29 k0=2.0e-31.*(T./300).^(-3.4);
30 kinf=2.9e-12.*(T./300).^(-1.1);
31 k=k0.*M./(1+(k0.*M./kinf)).*0.6.^((1+(log10(k0.*M./kinf)).^2).^(-1));
32 Y(HO2NO2) = 1;
33
34 HO2NO2;
35 eq=2.1e-27.*exp(10900/T);
36 k0=2.0e-31.*(T./300).^(-3.4);
37 kinf=2.9e-12.*(T./300).^(-1.1);
38 kf=k0.*M./(1+(k0.*M./kinf)).*0.6.^((1+(log10(k0.*M./kinf)).^2).^(-1));
39 k=kf./eq;
40 Y(HO2) = 1;
41 Y(NO2) = 1;
42
43 OH + HO2NO2;
44 k=4.71e-12;
45 Y(HO2) = 1;
46 Y(NO2) = 1;
47
48

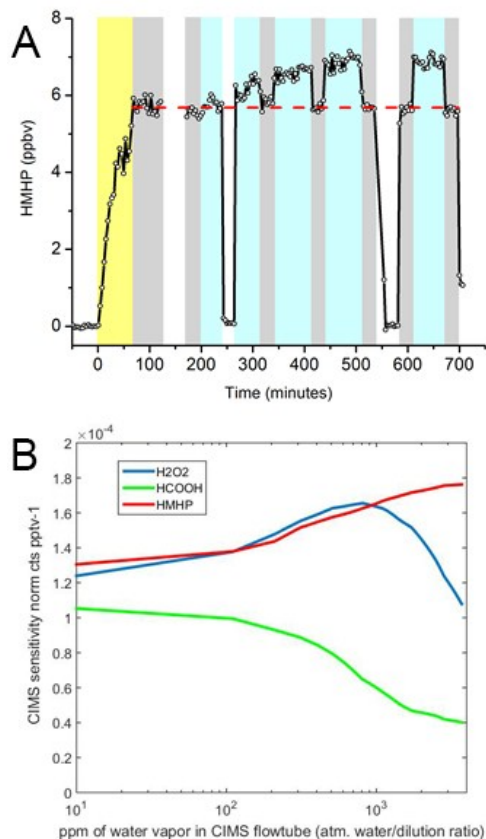
```

1 **Scheme S2:** Possible rearrangement of dioxiranes with allylic functionality.



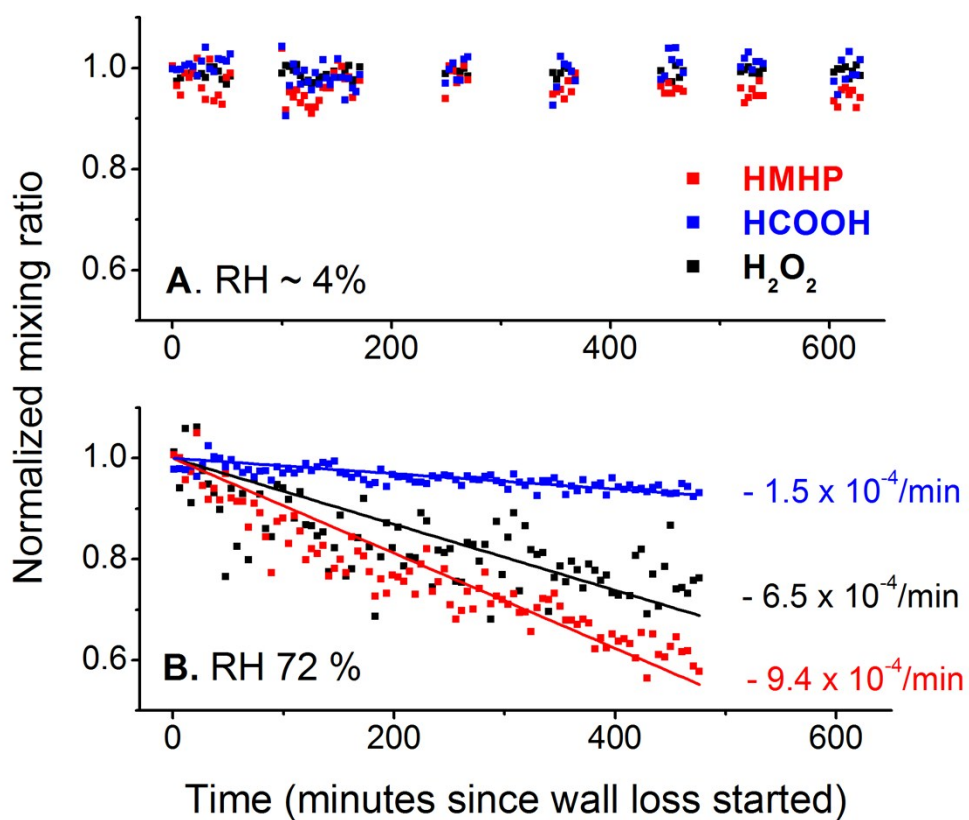
2

3



1

2 **Figure S1:** (A) Partial calibration of the humidity dependence of HMHP ion sensitivity in CIMS. The
 3 $\text{HO}_2 + \text{HCHO}$ reaction (from the photolysis of 4ppmv of formaldehyde, yellow shaded region) was used
 4 to produce approximately 5.7 ppbv of HMHP in the atmospheric chamber at 298K and 1 atm. The HMHP
 5 mixing ratio was allowed to stabilize for 1 hour before water-dependent calibration started. The stabilized
 6 HMHP mixing ratio from the chamber was sampled in the dark by CIMS, with nitrogen dilution streams
 7 that contained various mixing ratios of water: Gray regions denote 147 sccm of chamber air (dry) mixed
 8 with 1600 sccm of a dry ($[\text{H}_2\text{O}] < 100$ ppmv) nitrogen flow (similar to standard operation), blue regions
 9 denote 147 sccm of chamber air mixed with 1600 sccm of a humid ($[\text{H}_2\text{O}]$ up to 4000 ppmv) nitrogen
 10 flow, and white regions denote a break in sampling or sampling of 147 sccm of clean air mixed with 1600
 11 sccm of a dry nitrogen flow. Data from the gray regions were used to confirm that the mixing ratio of
 12 HMHP in the chamber did not change significantly throughout the calibration period. Data from the white
 13 regions were used to confirm that the background (free of HMHP) did not shift throughout the calibration
 14 period. (B) The complete relationship of CIMS ion sensitivity vs. water vapor in the CIMS flow region
 15 for H_2O_2 , HCOOH , and HMHP for the instrument used in this study.

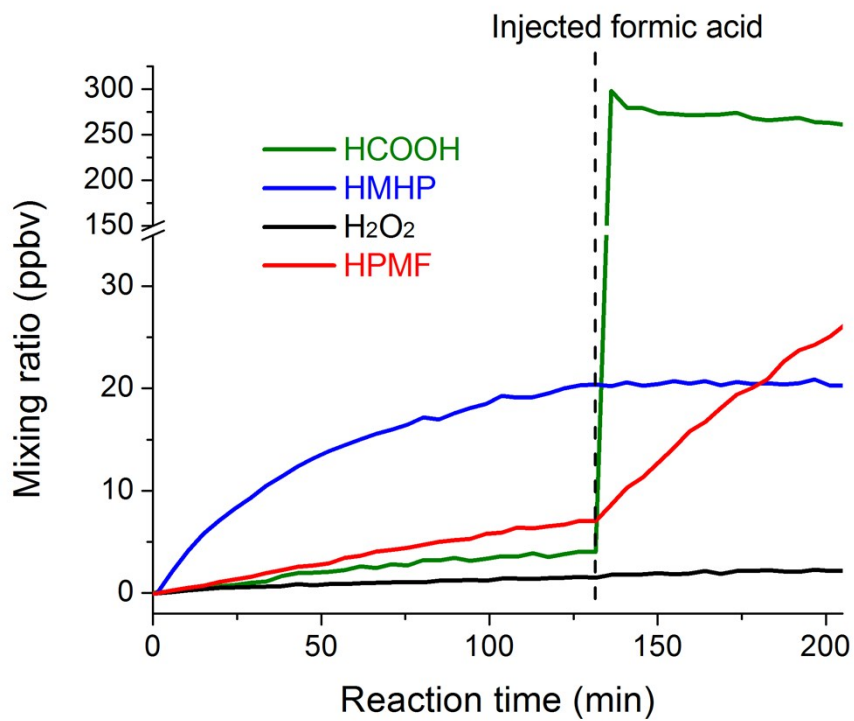


1

2

3 **Figure S2:** Wall loss rates of HMHP, HCOOH, and H₂O₂ at two representative relative humidity conditions.

4



1

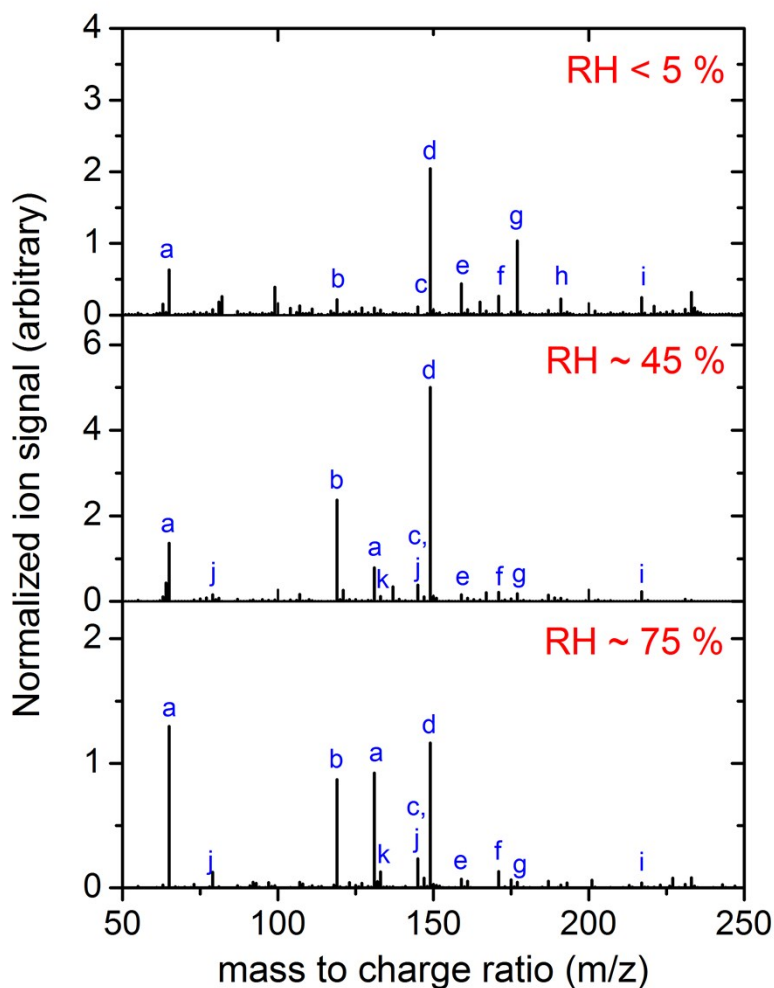
2 **Figure S3:** An ozonolysis experiment, where formic acid was injected halfway through the experiment.

3 The signal for HPMF was the only one (besides formic acid) that increased due to the reaction of CH₂OO

4 + HCOOH.

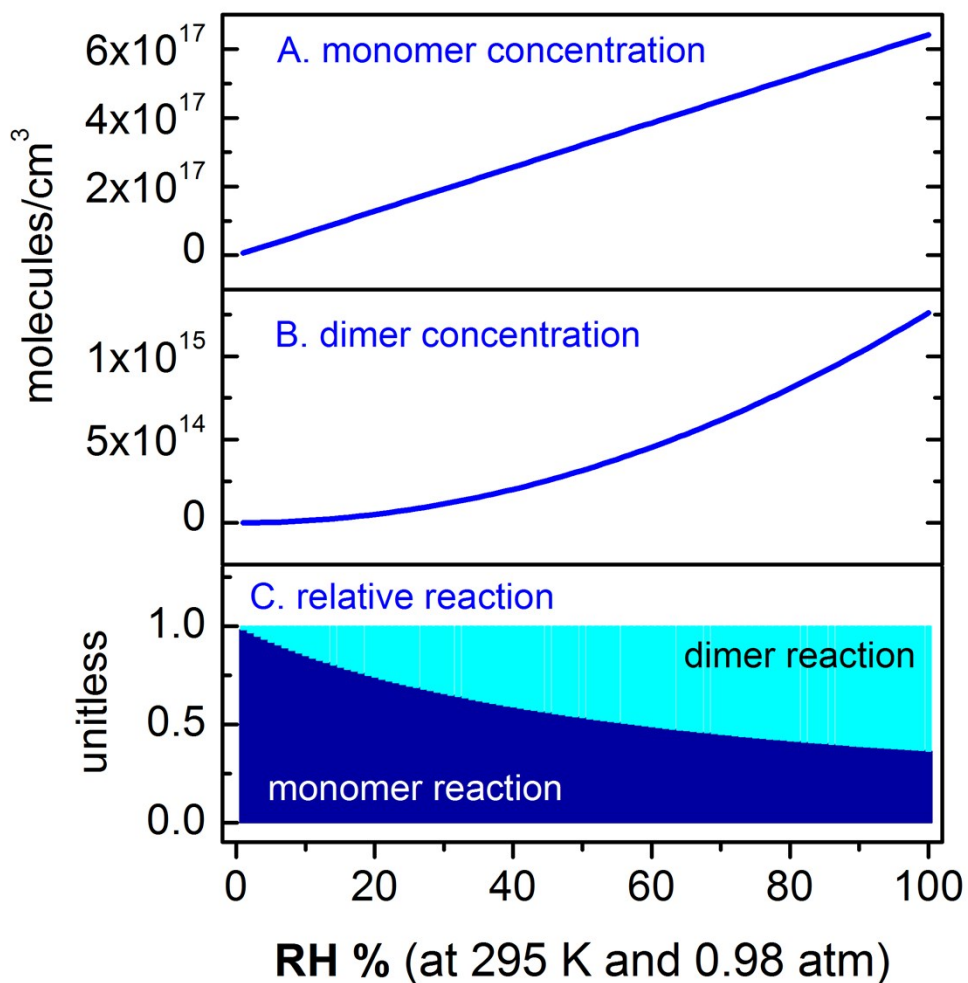
5

1



2

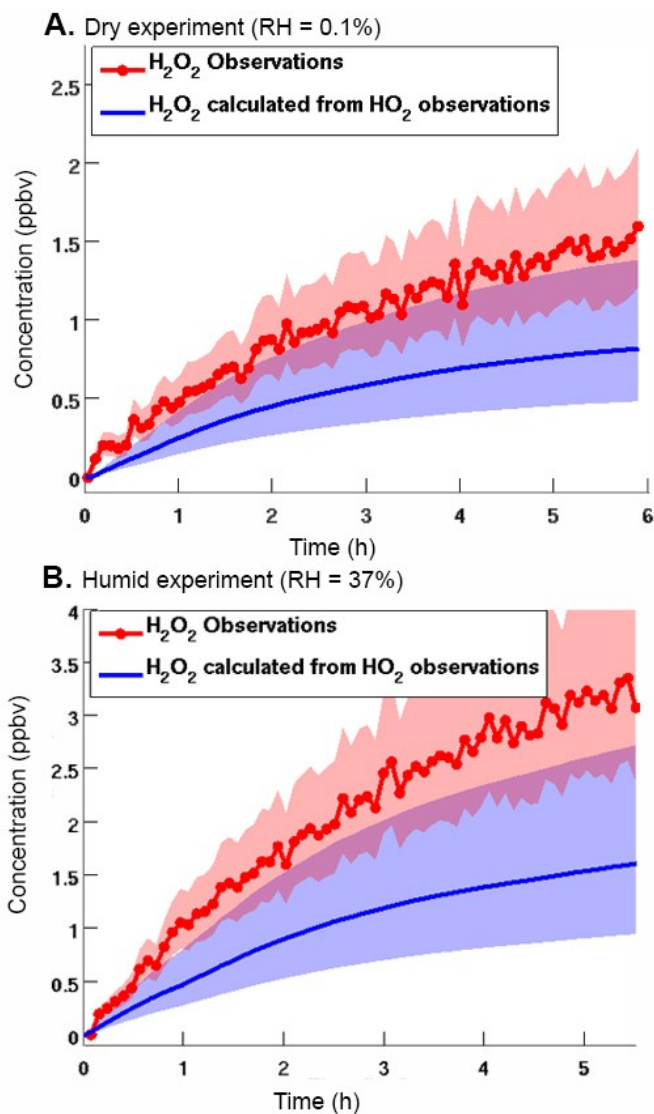
3 **Figure S4:** CF_3O^- CIMS mass spectra shown for three RH experiments. In general acidic compounds are
 4 quantified by their fluoride transfer ($\text{M} + \text{F}^-$) ion and most other compounds by the cluster ion ($\text{M} + \text{CF}_3\text{O}^-$
 5). Each compound has a water-dependent calibration that has not been applied to the figure, so the ion
 6 signals should be interpreted qualitatively. The peak labels correspond to: (a) $\text{HCOOH} - m/z$ 65 (transfer)
 7 and m/z 131 (cluster), (b) $\text{H}_2\text{O}_2 - m/z$ 119 (cluster), (c) Glycolaldehyde or isobaric compound - m/z 145
 8 (cluster), (d) HMHP - m/z 149 (cluster), (e) Hydroxyacetone or methylvinylhydroperoxide - m/z 159
 9 (cluster), (f) Unidentified - m/z 171, (g) HPMF - m/z 177 (cluster), (h) Unidentified - m/z 191, (i)
 10 Unidentified - m/z 217, (j) Acetic acid - m/z 79 (transfer) and m/z 145 (cluster), (k) Methyl hydroperoxide
 11 - m/z 133 (cluster). Peaks from CF_3O^- reagent have been subtracted and suspected impurities are not
 12 labelled. Glycolaldehyde and acetic acid cluster (m/z 145) are isobaric; however, the m/z 145 signal is
 13 mainly due to glycolaldehyde at low RH and acetic acid at higher RH (confirmed by a corresponding
 14 transfer ion).



1

2 **Figure S5:** The population of (A) water monomer molecules and (B) water dimer molecules as a function
 3 of RH, based on cluster association equilibrium thermodynamic functions reported in Ref.¹ The fraction of
 4 each reaction, using rate coefficients reported in the main text and in Scheme S1, is shown in panel C.

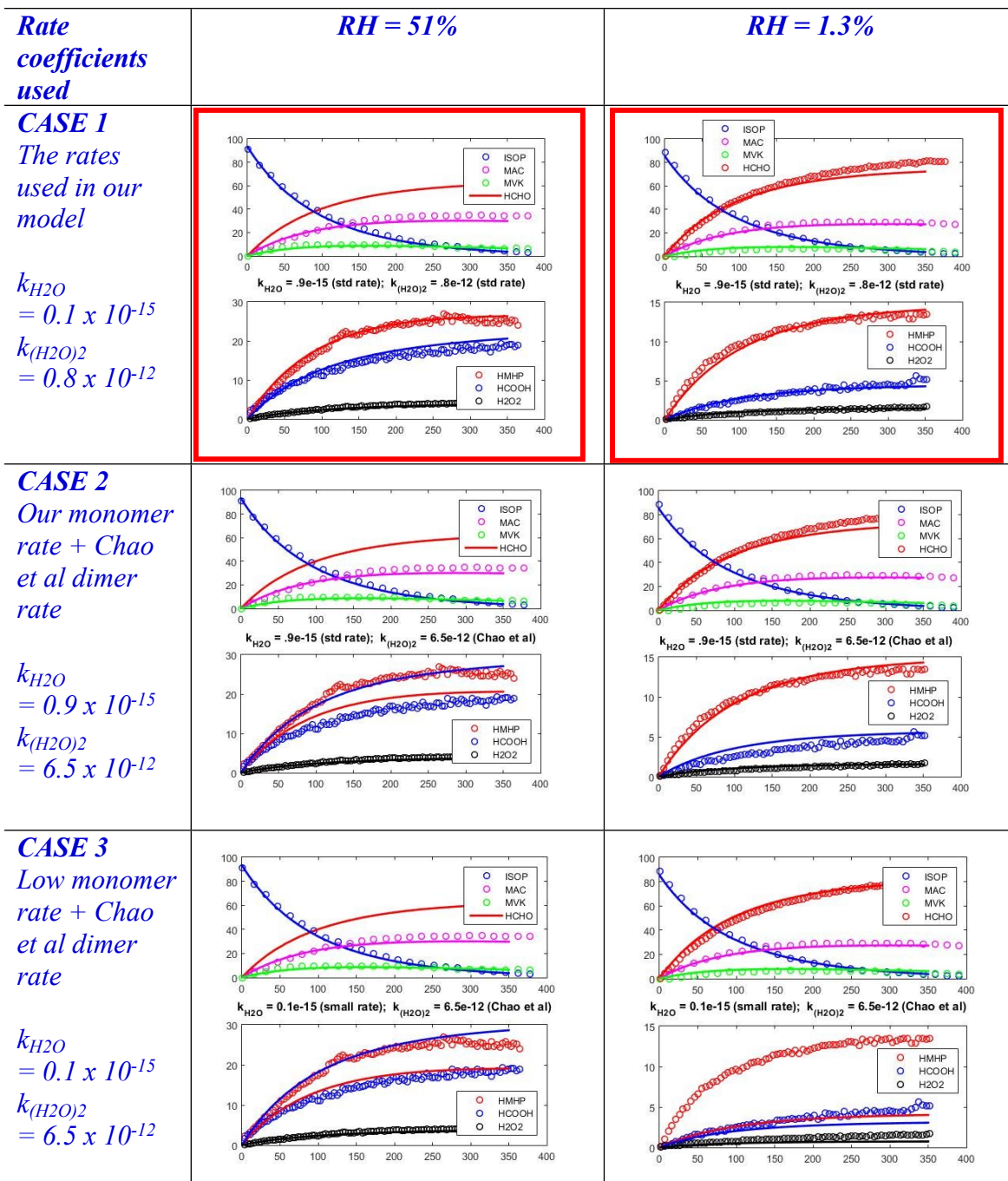
5



1

2 **Figure S6:** Comparison between H₂O₂ observed by CIMS (filled markers) and calculated H₂O₂
 3 using observed HO₂ data from GTHOS (Fig. S8, lines) for (A) dry conditions, $k_{\text{HO}_2+\text{HO}_2, 295\text{K}} = 2.92$
 4 $\times 10^{-12} \text{ cm}^3 \text{ molec}^{-1} \text{ s}^{-1}$ and (B) RH 37% conditions, $k_{\text{HO}_2+\text{HO}_2, 295\text{K}} = 3.53 \times 10^{-12} \text{ cm}^3 \text{ molec}^{-1} \text{ s}^{-1}$.
 5 Uncertainty bounds are used as reported in the main text. Rate coefficients are derived the
 6 temperature and RH dependence reported by Stone and Rowley (2005).²

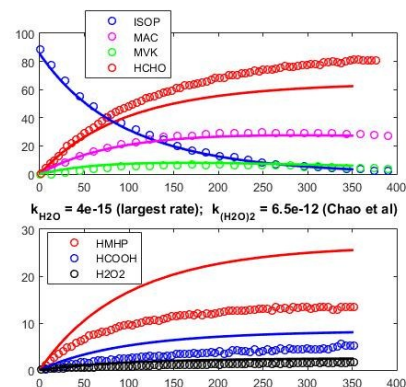
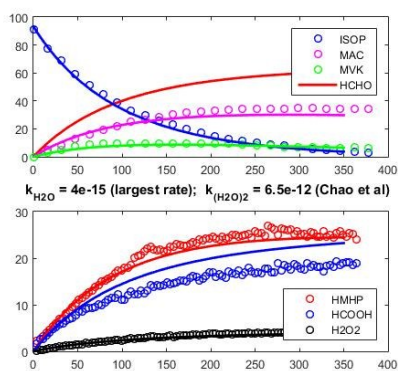
7



CASE 4
High Welz et al maximum monomer rate + Chao et al dimer rate

$$k_{H_2O} = 4 \times 10^{-15}$$

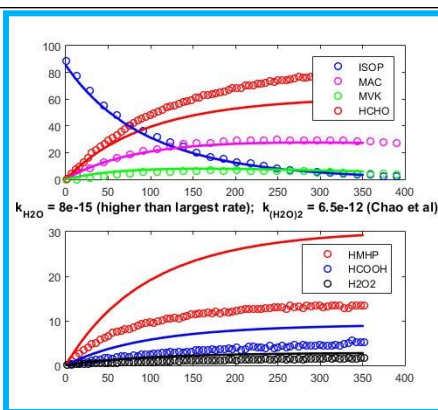
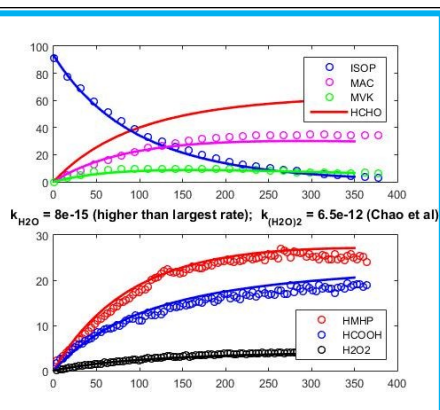
$$k_{(H_2O)_2} = 6.5 \times 10^{-12}$$



CASE 5
Unreasonably high monomer rate + Chao et al dimer rate

$$k_{H_2O} = 8 \times 10^{-15}$$

$$k_{(H_2O)_2} = 6.5 \times 10^{-12}$$

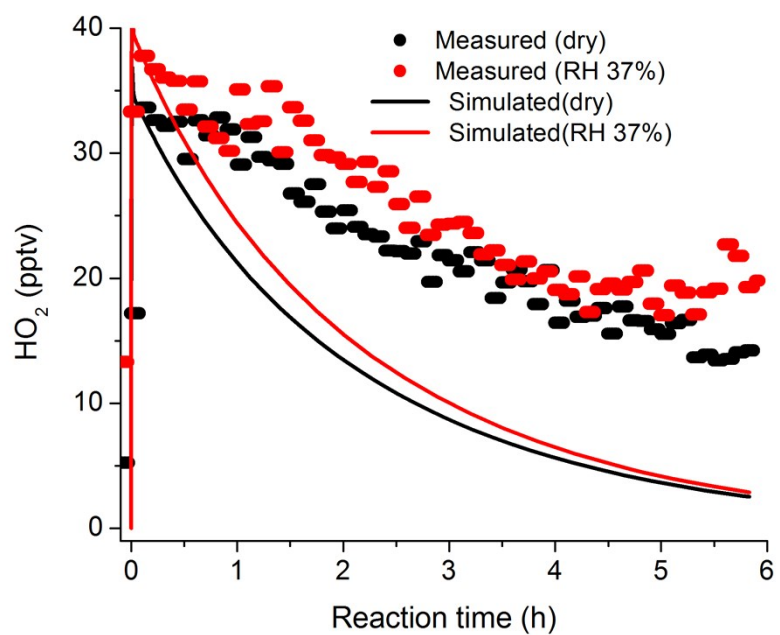


1

2 **Figure S7:** Model sensitivity study using two RH conditions (RH = 51%, where the water dimer and
 3 water monomer rate are both important, and RH = 1.2%, where only the water monomer rate is
 4 important). Results from 5 sensitivity cases, using different monomer and dimer rate coefficients, are
 5 shown. Case #1, shown in the red border, successfully reproduces all data reported in this work (Figure 5
 6 in the manuscript). Cases 2-5 explored the dimer rate coefficient of Chao et al (2015). For the Chao et al.
 7 (2015) dimer rate coefficient to reproduce the RH = 51% results, the monomer rate coefficient would
 8 need to be adjusted to be higher than the upper bound reported by Welz et al. (2012) – shown in the blue
 9 border, Case #5. The high monomer rate in Case #5 now over predicts CH₂OO water products in the dry
 10 case.

11

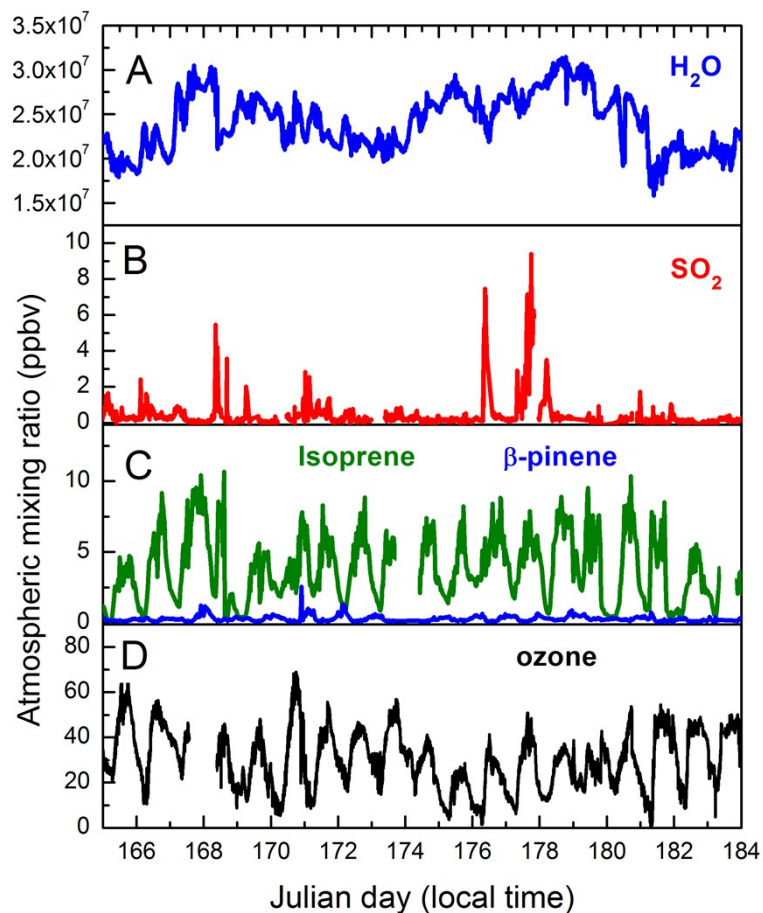
12



1

2 **Figure S8:** Simulated and measured HO₂ mixing ratios at two RH conditions during the FIXCIT
3 campaign. The model mechanism does not yet include second-generation sources of HO₂.

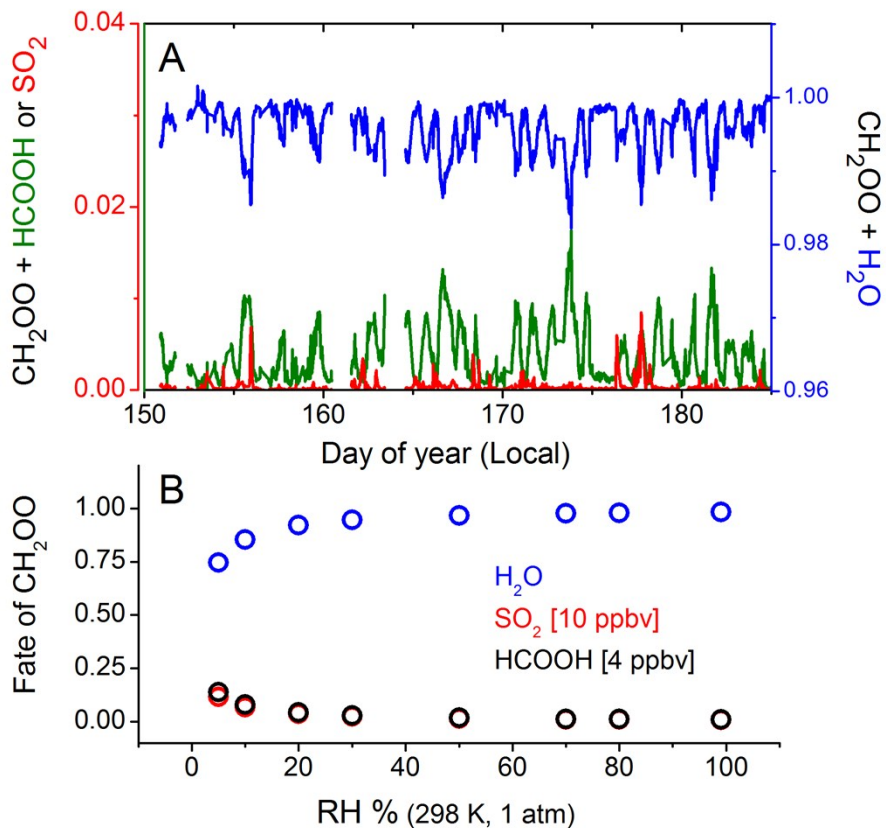
4



1

2 **Figure S9:** Atmospheric mixing ratios of (A) water vapor, (B) sulfur dioxide, (C) exocyclic VOCs isoprene
 3 and beta-pinene, and (D) ozone during the measurement period of the SOAS campaign.

4



1

2 **Figure S10:** (A) Fraction of CH_2OO that reacts with H_2O , SO_2 and HCOOH during the SOAS campaign.
 3 (B) Given high SO_2 and HCOOH mixing ratios, the fate of CH_2OO varies with RH; however, the H_2O
 4 reaction dominates at all realistic atmospheric humidities.

5

6 References:

- 7 1. J. C. Owicki, L. L. Shipman and H. A. Scheraga, *J. Phys. Chem.*, 1975, 79, 1794-1811.
 8 2. D. Stone and D. M. Rowley, *Phys. Chem. Chem. Phys.*, 2005, 7, 2156-2163.

9